Received: 30 January 2020 | Accepted: 11 April 2020
DOI: 10.1002/hyp.13780

WILEY

RESEARCH ARTICLE

Non-linear quickflow response as indicators of runoff generation mechanisms

Charles I. Scaife[1] | Nitin K. Singh[2] | Ryan E. Emanuel[3] | Chelcy Ford Miniat[4] | Lawrence E. Band[1,5]

[1]Department of Environmental Sciences, University of Virginia, Charlottesville, Virginia

[2]Geosciences and Geological and Petroleum Engineering, Missouri University of Science and Technology, Rolla, Missouri

[3]Department of Forestry and Environmental Resources, North Carolina State University, Raleigh, North Carolina

[4]Coweeta Hydrologic Laboratory, Southern Research Station, USDA Forest Service, Otto, North Carolina

[5]Department of Engineering Systems and Environment, University of Virginia, Charlottesville, Virginia

Correspondence
Charles I. Scaife, Department of Environmental Sciences, University of Virginia, Charlottesville, Virginia 22904, USA.
Email: cis9zg@virginia.edu

Funding information
Division of Biological Infrastructure, Grant/Award Number: DBI1226983; Division of Earth Sciences, Grant/Award Numbers: EAR-0725019, EAR-1239285, EAR-1331726; Division of Environmental Biology, Grant/Award Numbers: DEB0218001, DEB0823293, DEB1440485, DEB1637522, DEB8012093, DEB8706444, DEB9011661

Abstract

Linking quickflow response to subsurface state can improve our understanding of runoff processes that drive emergent catchment behaviour. We investigated the formation of non-linear quickflows in three forested headwater catchments and also explored unsaturated and saturated storage dynamics, and likely runoff generation mechanisms that contributed to threshold formation. Our analyses focused on two reference watersheds at the Coweeta Hydrologic Laboratory (CHL) in western North Carolina, USA, and one reference watershed at the Susquehanna Shale Hills Critical Zone Observatory (SHW) in Central Pennsylvania, USA, with available hourly soil moisture, groundwater, streamflow, and precipitation time series over several years. Our study objectives were to characterise (a) non-linear runoff response as a function of storm characteristics and antecedent conditions, (b) the critical levels of shallow unsaturated and saturated storage that lead to hourly flow response, and (c) runoff mechanisms contributing to rapidly increasing quickflow using measurements of soil moisture and groundwater. We found that maximum hourly rainfall did not significantly contribute to quickflow production in our sites, in contrast to prior studies, due to highly conductive forest soils. Soil moisture and groundwater dynamics measured in hydrologically representative areas of the hillslope showed that variable subsurface states could contribute to non-linear runoff behaviour. Quickflow generation in watersheds at CHL were dominated by both saturated and unsaturated pathways, but the relative contributions of each pathway varied between catchments. In contrast, quickflow was almost entirely related to groundwater fluctuations at SHW. We showed that co-located measurements of soil moisture and groundwater supplement threshold analyses providing stronger prediction and understanding of quickflow generation and indicate dominant runoff processes.

KEYWORDS
antecedent soil moisture, Appalachian Mountains, emergent behaviour, forested catchments, piecewise linear regression, rainfall intensity, riparian groundwater wells, storage–flux relationships

1 | INTRODUCTION

Capturing physical runoff processes that explain the formation of emergent hydrologic properties has been a major goal of runoff threshold research; however, emergent properties by their nature integrate over several non-linear, co-occurring processes rather than individual runoff generation mechanisms. This includes mechanisms of saturated throughflow (Hewlett & Hibbert, 1967), expansion of variable source areas (Dunne & Black, 1970), flow through soil pipes and macropores (Mosley, 1979, 1982), flow at the soil–bedrock interface (McDonnell, 1990; Weiler & McDonnell, 2004), or rainfall excess overland flow (Horton, 1933). Runoff processes also have high spatiotemporal variability ranging several orders of magnitude from seconds to years and from soil pores to hillslopes. This process complexity is partially explained by catchment properties like soil type (e.g., Wilson et al., 2017), geologic substrate (e.g., Fu, Chen, Jiang, & Dong, 2013), land use (e.g., Ramos-Scharrón & LaFevor, 2018), and climate; however, bottom-up hydrologic prediction using mechanistic models remains difficult without the calibration of several parameters to achieve flow fidelity (Hrachowitz et al., 2013). Alternatively, top-down estimates of runoff may be empirically derived from simpler relationships between hydrologic fluxes and catchment storage of water (Wittenberg & Sivapalan, 1999). Models of emergent hydrologic behaviour can be developed through the spatiotemporal integration of moisture storage states and runoff processes across the entire catchment (Duffy, 1996; Kirchner, 2009; Teuling, Lehner, Kirchner, & Seneviratne, 2010), but a major question is whether or not there are signatures of specific runoff generation mechanisms in non-linear quickflow response.

Non-linear quickflow response has broadly been linked to catchment connectivity (Buttle, Dillon, & Eerkes, 2004; Lehmann, Hinz, McGrath, Meerveld, & McDonnell, 2007) through mechanisms like fill-and-spill and flow along soil–bedrock interfaces (Freer et al., 2002; Spence & Woo, 2003), hillslope connection to riparian areas (Jencso et al., 2009; McGlynn, McDonnell, Seibert, & Kendall, 2004), lateral pipe flow activation (Meerveld & McDonnell, 2006b; Uchida, Kosugi, & Mizuyama, 2001; Uchida, Meerveld, & McDonnell, 2005), and transmissivity feedbacks in the deeper subsurface (Detty & McGuire, 2010), but separating out the primary fluxes contributing to non-linear behaviour from several co-occurring runoff processes is challenging and requires intensive measurement. For example, in Watershed 3 of Hubbard Brook Experimental Forest in New Hampshire, Detty and McGuire (2010) used a large network of groundwater wells to show negligible contributions of both saturation and infiltration-excess overland flow common in variable source area (VSA) models. Instead, rising groundwater levels became asymptotic with increasing stormflow generation indicating rapid drainage from a highly conductive soil layer. These transmissivity feedbacks were greater during large storms when hillslope wells were also activated and connected to the riparian area. Intensive trench experiments conducted across humid, forested catchments in Georgia, USA (Meerveld & McDonnell, 2006a) and in Japan (Uchida et al., 2005) found rain event size determined hillslope activation via measurements of pipeflow.

Saffarpour, Western, Adams, and McDonnell (2016) used a multiple thresholds analysis to identify critical values of subsurface and storm conditions that may be indicative of specific runoff processes rather than measuring the processes themselves. Like previous studies, they found that the sum of gross precipitation and antecedent soil moisture was a major control on quickflow response. However, maximum hourly rainfall was a secondary control in their grassland catchment. Under dry antecedent conditions, a small but intense storm can trigger quickflow via infiltration excess overland flow or preferential flows that contribute to rising groundwater. Few studies in humid forested catchments use threshold analysis of input variables to explore runoff processes and quickflow generation using empirical measurements of subsurface state and storm characteristics. In forested catchments, the capacity to absorb the effects of high intensity storms is also well-documented. Hewlett, Fortson, and Cunningham (1984) tested the effects of rainfall characteristics, soil wetness conditions, and seasonality on stormflow in 15 undisturbed and mostly forested headwater catchments. They found that maximum rainfall intensity had a negligible effect on peak flows and total runoff depths.

A major challenge of examining dominant runoff mechanisms across catchments is the intensity of measurement required. Rather than intensively sampling across catchments or installing hillslope trenches, we make use of hydrologically representative sites, which may reveal subsurface dynamics pervasive across the catchment. In particular, these hydrologically representative sites can have temporal soil moisture patterns correlating to mean hillslope response (Grayson & Western, 1998; Vachaud, Silans, Balabanis, & Vauclin, 1985) or aggregate sufficiently large upslope areas achieving a steady state relationship between groundwater storage and streamflow (Seibert, Bishop, Rodhe, & McDonnell, 2003). The correlation lengths between measurements of groundwater or soil moisture can be on the order of tens of metres (Brocca, Morbidelli, Melone, & Moramarco, 2007) depending on hillslope length making it vital to reduce spatial offsets between streams, groundwater wells, and soil moisture plots. Applying a multiple threshold analysis, as discussed above, to measurements of groundwater and soil moisture made at hydrologically representative sites may reveal differences in runoff processes even among seemingly similar basins without implementing intensive hillslope measurements.

Soil moisture and groundwater data may be used to supplement threshold analyses revealing mechanisms of runoff generation contributing to rapidly rising flows. In this study, our objectives were to characterise (a) non-linear runoff response as a function of storm characteristics and antecedent conditions, (b) the critical levels of shallow unsaturated and saturated storage that lead to hourly flow response, and (c) runoff mechanisms contributing to non-linear quickflow using the wetness of the shallow unsaturated zone relative to the saturated zone in three forested, control catchments. We leveraged high-resolution hydrometric and climatological data collected by the Long-Term Ecological Research and Critical Zone Observatory sites in small forested, headwater catchments in the Southern and Central Appalachian Mountains. Using co-located soil moisture and groundwater measurements, we characterized the impacts of

subsurface storage on hourly flows and discussed runoff generation mechanisms contributing to flow. We hypothesised that (a) non-linear runoff response was a function of antecedent soil moisture and rainfall depth but not rainfall intensity, (b) that the combination of wetter shallow soil moisture and higher groundwater water tables generally corresponded to greater quickflows across our catchments, and (c) runoff mechanisms contributing to quickflow response originated from both shallow and deeper subsurface drainage.

2 | MATERIALS AND METHODS

2.1 | Site description

Study sites were located in forested catchments in the Appalachian Mountains (Figure 1, Table 1). Watersheds 2 and 14 were located at the Coweeta Hydrologic Laboratory (hereafter, CHL) in the southern Appalachian Mountains of western North Carolina, USA, and a third catchment was located at the Susquehanna Shale Hills Critical Zone Observatory (hereafter, Shale Hills) in the central Appalachian Mountains in central Pennsylvania. CHL is a USDA Forest Service experimental forest and a National Science Foundation (NSF) Long-Term Ecological Research (LTER) site composed of experimental and reference watersheds that were established in the 1930s. Shale Hills was established in the 1950s in the Stone Valley Forest owned by Pennsylvania State University before joining the NSF Critical Zone Observatory network in 2007.

Climate at CHL and Shale Hills is classified as marine, humid temperate under Köppen's climate classification system and is characterised by frequent rainfall that is evenly distributed throughout the year (Swift Jr., Cunningham, & Douglass, 1988). For our analysis, data from Watershed 2 (WS2) and Watershed 14 (WS14) at CHL and from a single watershed at Shale Hills (SHW) were used. Precipitation incident on the Coweeta Basin is strongly influenced by orography (Burt, Miniat, Laseter, & Swank, 2018); however, within the low elevation and relatively low relief (<300 m) catchments of WS2 and WS14, orographic effects are

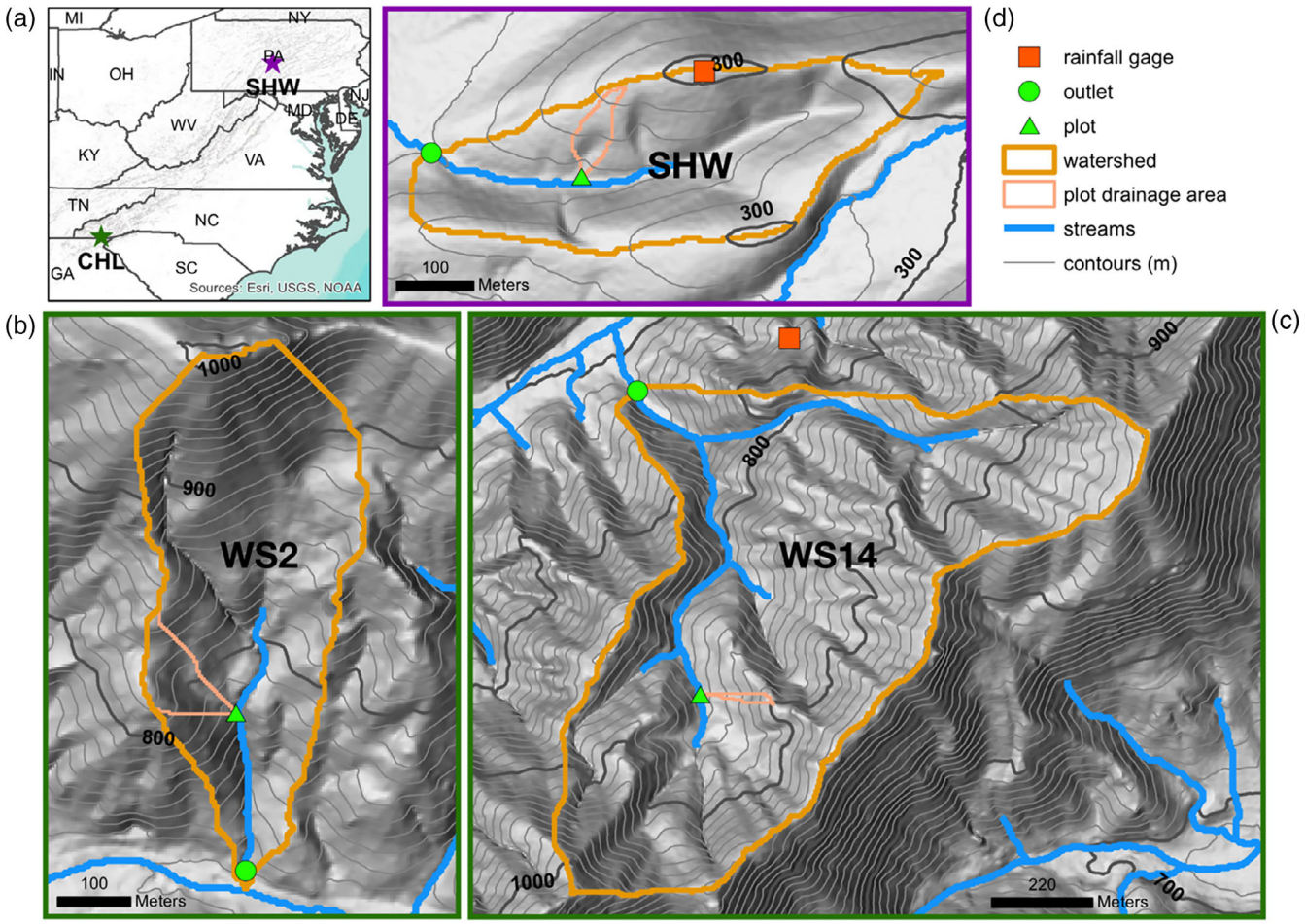

FIGURE 1 (a) The Coweeta Hydrologic Laboratory (35°03′35″N, 83°25′49″W) in western North Carolina and Susquehanna Shale Hills Critical Zone Observatory (40°39′52″N, 77°54′19″W) in Central Pennsylvania are both situated in Appalachian Mountains. The three reference catchments used in this study were (b) Watershed 2 (WS2), (c) WS14 and (d) Shale Hills Watershed (SHW). Plots where hourly soil moisture and groundwater were measured are shown above as green triangles along with upslope area draining to that plot. Hourly discharge (green circles) was measured at the outlet of each catchment, and hourly precipitation was measured at climate stations (orange squares)

TABLE 1 Summary of study site properties and climate of WS2 and WS14 at CHL and of SHW at Shale Hills

	WS2	WS14	SHW
Landcover	Forested, control	Forested, control	Forested, control
Aspect	South	North	West
MAP (mm)[a]	1,996 ± 437	1,996 ± 437	1,090 ± 214
Watershed area (ha)	13	62.4	8
Relief (m)	298	285	54
Average slope (deg)	28.8	27.3	15.1/19.8[b]

[a]Mean annual precipitation, years calculated 1/2011–12/2014 (CHL) and 1/2009–12/2011 (SHW).
[b]North-facing/south-facing.

negligible. Similarly, the relief at SHW is only 54 m and imparts no orographic effect. Rainstorms vary throughout the year in both study locations and tend to be more convective in the summer and more frontal in the winter (Laseter, Ford, Vose, & Swift, 2012; Miller, Miniat, Wooten, & Barros, 2019). At CHL, spatial patterns of rainfall are reinforced more strongly by elevation during the summer months (Daly, Slater, Roberti, Laseter, & Swift, 2017), likely due to convective storms generating over higher elevations.

WS2 at CHL is a 13 ha south-facing catchment and WS14 is a 62.4 ha north-facing catchment. Both watersheds feature mixed oak and cove hardwood dominated stands with an ericaceous evergreen shrub layer dominated by *Kalmia latifolia* and *Rhododendron maximum* (Day, Phillips, & Monk, 1988; Elliott, Vose, Swank, & Bolstad, 1999). The soils at CHL are sandy loam Inceptisols and Ultisols (Velbel, 1988) underlain by gneiss and schist formations (Hatcher, 1988). Average soil conductivities observed in nearby deeply, weathered soils were 63 mm hr^{-1} (Price, Jackson, & Parker, 2010) and regolith depth was roughly 7 m (Swank & Douglass, 1975). Shallow groundwater wells installed for this study had completion depths between 0.9 and 3.5 m (Singh, Emanuel, Nippgen, McGlynn, & Miniat, 2018b). The south-facing WS2 has a greater potential evapotranspiration rate than the north-facing WS14, evinced by the annual runoff ratio of 0.45 in the former and 0.53 in the latter (Nippgen, McGlynn, Emanuel, & Vose, 2016).

SHW is an 8 ha west-facing catchment with predominantly north-/south-facing slopes that are less steep than CHL (Brantley et al., 2019). Five dominant soil types occupy distinct topographic positions at SHW with decreasing soil moisture storage with distance to stream. Soils are predominately silt loam transitioning to silt clay loam with depth (Lin, 2006) and underlain by shale (Berg et al., 1980). Soil conductivities measured in riparian areas varied between 22.8 and 142.2 mm hr^{-1} (Lin, Kogelmann, Walker, & Bruns, 2006). Median depth to bedrock ranges from roughly 40 cm to 1 m depending on soil type and soils tend to be deeper on south-facing hillslopes (Lin et al., 2006). Stands are dominated by mature oaks, which compose 64% of the basal wood area (Brantley et al., 2019). The remaining vegetation includes species of maple, hickory, and pine in addition to eastern hemlock (Smith, Eissenstat, & Kaye, 2017). The average annual runoff ratio computed from 2009 to 2010 was 0.44.

2.2 | Hydrometric measurements

At CHL, stream stage was measured every 5 min at the outlets of WS2 and WS14 using 90° and 120° v-notched weirs, respectively, and converted to units of discharge using rating equations (Swift Jr. et al., 1988). At SHW, stream stage was measured at the outlet every 1 min using a double *v*-notched weir and integrated to 10 min intervals before being converted into discharge using rating curves. Two precipitation gages located near WS14 were used for both CHL catchments to estimate total rainfall depth (SRG41, 8-in Standard Rain Gauge, National Weather Service) and rainfall intensity and duration (RRG41, Belfort Universal Recording Rain Gauge, Belfort Instrument Co., Baltimore, MD) measured at 5 min intervals. The precipitation gage at SHW (OTT Pluvio^2, Kempten, Germany) was located near the catchment ridge and measured rainfall at 10 min intervals (Figure 1).

Within each catchment, plots were established to measure soil moisture and groundwater level as part of several independent studies. As such, instruments and plots were not coordinated across studies. Nine soil moisture plots across three hillslope catena, each with a down-, mid-, and upslope positions, were established in WS2. Soil moisture was measured at 10, 20, 30, 60, and 100 cm depths using reflectometry probes (CS625, Campbell Scientific, Logan, UT) inserted horizontally into the soil (Singh et al., 2018b). Piezometer groundwater wells were installed in down- and midslope positions for all three hillslopes in WS2, and water level was measured at 30 min intervals (WT-HR, TruTrack, Inc., Christchurch, New Zealand). WS14 had soil moisture and groundwater plots established in three transects along a single hillslope spanning from the stream to the ridge. Continuous measurements were made in a single transect in sites closest to the stream. At each site, soil moisture was measured at 30 and 60 cm at 1 min intervals using reflectometry soil moisture probes inserted vertically (CS625, Campbell Scientific, Logan, UT). Piezometer groundwater wells in WS14 measured groundwater level at 1 min intervals (CS450, Campbell Scientific, Logan, UT) and were co-located with soil moisture measurements. At SHW, three plots were established in a triangular cluster near the stream. Within each plot, soil moisture was measured at 10, 30, and 50 cm depths using capacitance soil moisture probes (Echo2 EC20, Decagon Devices, Inc., Pullman, WA) and three piezometer groundwater wells were established nearby (CS420-L,

Campbell Scientific, Logan, UT). Soil moisture and groundwater level were measured at 10 min intervals.

2.3 | Data analysis

Criteria for selecting soil moisture and groundwater instrument pairs within each catchment were based on the percent of continuous data and the topographic location of each plot. In general, the most downslope sites were selected for two reasons: (a) groundwater becomes decoupled from flow with increasing distance to stream (Seibert et al., 2003) and (b) downslope plots may aggregate the hydrologic behaviour of the upslope region draining to it. As a consequence, these sites were assumed to be more hydrologically representative of hillslope scale or, in some cases, catchment scale dynamics. Strengthening our case for using downslope plots in WS2 and WS14 was the discontinuous record of groundwater levels at midslope positions due to unresponsive or dry wells. At SHW, all sites were located on the valley floor, so wells were never dry; however, sufficient temporal coverage of soil moisture data was limited to a single site.

Discharge and precipitation data were provided at hourly timesteps. At CHL, spatial variation of rainfall within low elevations catchments was assumed to be negligible at hourly timesteps. For our study, we aggregated subhourly soil moisture and groundwater data to match this temporal resolution by taking the mean. The period of analysis varied by site according to data availability (Table 2). At CHL, WS14 had continuous measurements from June 2011 to October 2014 encompassing measurements made in WS2 from October 2011 to December 2013. The mean monthly air temperature in WS14 over this period ranged between 2.9 and 22.8°C. As a result, most precipitation occurred as rain even during the winter. The period of analysis captured a water year with average rainfall in 2012 followed by one of the wettest years on record in 2013. In that wet year, baseflows from WS2 and WS14 were elevated and runoff responses to storm events were relatively larger compared to 2012 (Figure 2b). The measurement period at SHW was between January 2009 and January 2012 and mean monthly air temperature over this period was between −8.9 and 21.5°C such that roughly 6.5% of annual precipitation totals fell as snow. Our analysis period at SHW captured similar variation between dry years (2010 and 2011) and a wet year (2012). During particularly dry periods, the weir at SHW measured zero flow, most notably between July and October in 2010.

Storm events were defined as beginning with rainfall and accumulating at least 5 mm of rain, with a minimum peak hourly intensity of at least 1.5 mm hr^{-1}. Individual storms were separated by at least 12 hr. Quickflow was computed using the constant slope hydrograph method (Hewlett & Hibbert, 1967) written in MATLAB (The Mathworks Inc., Natwick, MA). Storm events that produced quickflow ended when quickflow returned to zero or the storm length reached 96 hours. This method is similar to Saffarpour et al. (2016) and allowed us to examine rain events that produced very little or no quickflow response, which was common during dry periods. Rainfall intensity was computed as the maximum hourly intensity over the entire storm event. Using our storm definition method, we identified 391 storms in total across all watersheds (Table 2).

To characterise thresholds in quickflow response, we followed previous studies that combined gross precipitation (gross p, mm) and antecedent soil moisture index (ASI, unitless; Saffarpour et al., 2016; Scaife & Band, 2017; Detty & McGuire, 2010). ASI was computed as an index that integrated soil moisture with depth (Haga et al., 2005), converting units of volume per volume to mm. Because soil moisture measurement depths varied across our study locations, we characterised soil moisture within the top 50 cm reflecting the depth of our shallowest site in SHW. Thresholds in quickflow response were assessed with respect to maximum hourly rainfall intensity and the sum of Gross p and ASI (Gross p + ASI) using a piecewise regression analysis (PRA). Following previous analyses (Buttle, Webster, Hazlett, & Jeffries, 2019), the *segmented* package in *R* (R Core Team, 2019; Muggeo, 2003) was used to quantitatively compute breakpoints (i.e., thresholds) and slopes. Due to the spatially heterogenous nature of soils, within catchment values of ASI varied as much as between catchment values. For this reason, our analysis focused on relative threshold behaviour within catchments and subsurface dynamics with respect to quickflow response rather than their absolute values. We also examined the simultaneous effects of maximum hourly rainfall intensity and Gross p + ASI on quickflow production by testing for multiple thresholds.

Using shallow subsurface measurements, we examined how soil moisture and groundwater levels relate to greater quickflows and how they covary over storm events. We characterised the degree of coupling between soil moisture and groundwater response over the storm by computing the slopes between soil moisture and groundwater at storm initiation (t_0) and peak quickflow (t_{peak}). A two-sample t-test was performed on slopes to determine whether the degree of coupling differed between storm events below the threshold versus

TABLE 2 Summary of measurement period and storm characteristics from WS2 and WS14 at CHL and from SHW at Shale Hills

	WS2	WS14	SHW
Analysis period	10/2011–12/2013	6/2011–10/2014	1/2009–12/2011
Measurement days	823	1,221	1,250
Runoff ratio	0.36	0.43	0.68
Quickflow:Totalflow	0.14	0.11	0.38
Number of storms	96	171	124
Median stormflow duration (hours)	19	17	28.5

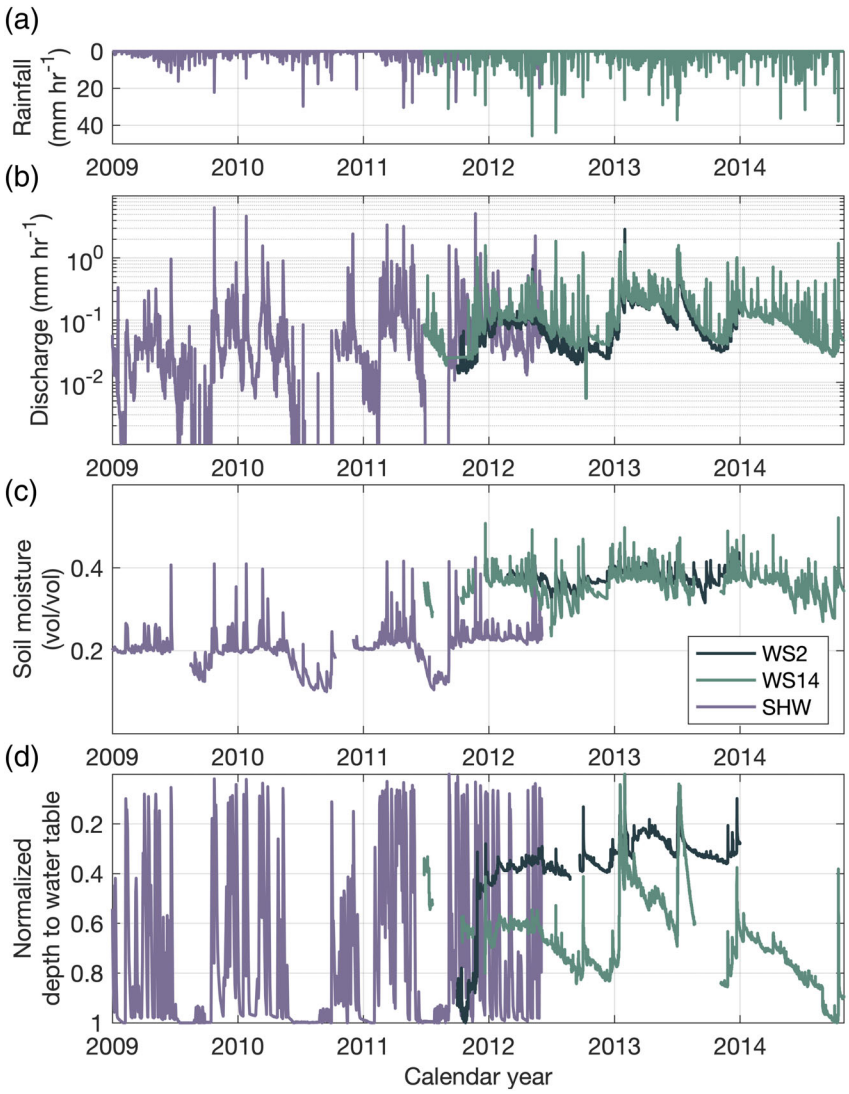

FIGURE 2 Time series of hourly hydrologic variables measured in each study catchment: (a) hourly rainfall depth at SHW and CHL, (b) log discharge in WS2, WS14, and SHW, (c) hourly soil moisture integrated with depth, and (d) hourly groundwater shown as a normalised depth to water table (mm)

storm events above the threshold. A simple ratio of soil moisture to groundwater was taken to represent the relative wetness states of the shallow unsaturated and saturated zones. This ratio was plotted as contours to further examine the degree of coupling during wetting and drying and was used directly as a predictor of quickflow. Lastly, we interpreted the dynamics of hourly response of soil moisture and groundwater to understand potential mechanisms contributing to flow on either side of the thresholds.

3 | RESULTS

3.1 | Stormflow response characteristics

Soil moisture dynamics over the study periods reflected seasonal and storm event scale variations. Seasonal shifts of soil moisture demonstrated large swings from dry, late growing season to wet, dormant season as reflected in SHW (Figure 2c). At CHL, WS2 and WS14 showed similar shifts from dry to wet states but to a lesser degree. At the storm event scale, sharp rises in soil moisture highlighted the responsiveness of soil moisture to precipitation. Of the three watersheds, WS2 had consistently greater soil moisture than SHW and WS14.

Median water table depths and responsiveness varied among sites (Figure S1, Figure 2d). The water table was deepest below the surface in WS14 and closest to the surface in SHW. Well response was also not consistent across our catchments. The range of measurements was much smaller in WS2 and WS14 (~400 mm and ~200 mm, respectively) compared to SHW (~800 mm). With the exception of SHW, groundwater never came within 500 mm of the surface where soil moisture is measured. Normalized groundwater levels in SHW were characterised by sharp peaks corresponding to storm events (Figure 2d). This effect was dampened or non-existent during the late growing season. In WS2 and WS14, groundwater levels recharged during the dormant season months and drained during the growing season months, but storm event variation was not as apparent at CHL.

Stormflow durations also differed among our catchment. SHW had the longest median stormflow duration lasting roughly 28.5 hr and median stormflow durations in WS14 and WS2 were 17 and

19 hr, respectively. The ratio of quickflow to total flow was greatest in SHW (0.38), whereas WS2 and WS14 were 0.14 and 0.11, respectively. Similarly, the runoff ratio was 0.68 in SHW and 0.36 and 0.43 over the measurement period in WS2 and WS14, respectively.

In all sites, quickflow depth was not as strongly correlated with ASI as it was with Gross *p* and maximum hourly rainfall intensity. Pearson correlation coefficients (ρ) were weak between ASI and quickflow depth ($\rho < 0.18$) in WS2 and WS14, but there was evidence of increasing quickflow depth variability with greater ASI (Figure 3a–c). In SHW, there was stronger evidence of a positive correlation between ASI and quickflow ($\rho = 0.30$). The relationship between quickflow and maximum hourly rainfall intensity was weak across all sites ($\rho \leq 0.46$), but stronger than the relationship between ASI and quickflow (Figure 3g–i).

Combining Gross *p* and ASI produced a non-linear quickflow relationship, but maximum hourly rainfall intensity did not impose a clear secondary threshold. Piecewise regression analyses reveal significant thresholds separating low quickflow sensitivity from high quickflow sensitivity with respect to Gross *p* + ASI (Figure 4; Table 3). The Gross *p* + ASI threshold was highest in WS2 (285 mm), followed by WS14 (182 mm) and SHW (124 mm). The slope parameters (m_1, m_2) varied by an order of magnitude between storms below and above the threshold (Table 3). The amount of quickflow produced during a storm event at CHL was not significantly dependent on the rainfall intensity but rainfall events that generated little to no quickflow typically had low maximum hourly rainfall intensity and small Gross *p* + ASI (Figure 5). At SHW, there was greater separation between events producing flow and no flow compared to WS2 and WS14 (Figure 5c). Given dry enough antecedent conditions, even large rainfall intensities could produce no flow.

3.2 | Subsurface response during storms

Hourly quickflow increased non-linearly with 0–50 cm soil moisture, but there was no consistent temporal pattern with groundwater levels

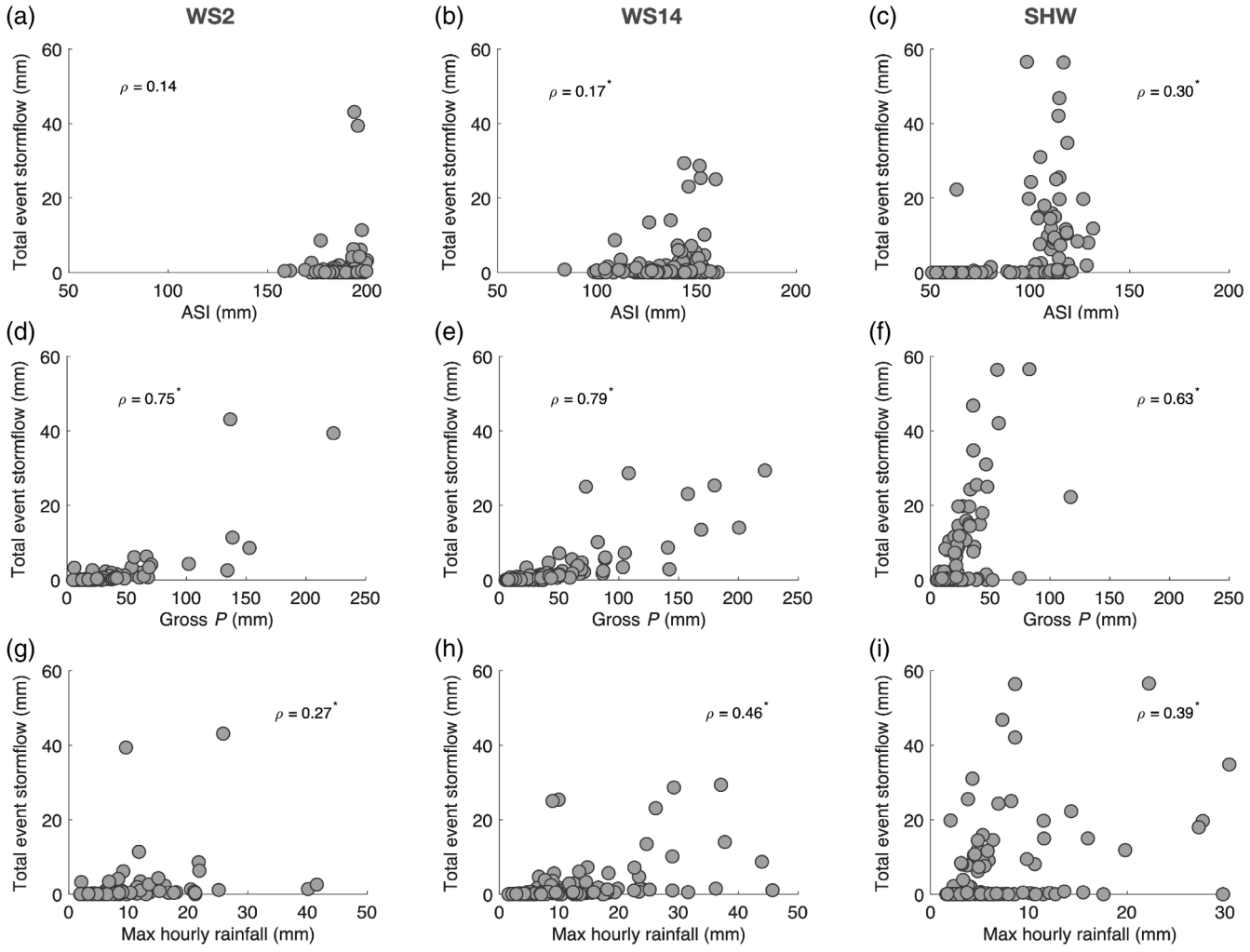

FIGURE 3 Total event stormflow generation as a function of ASI (a–c), gross precipitation (d–f), and max hourly rainfall (g–i) computed using hourly resolution data for WS2, WS14, and SHW. Pearson correlation coefficients (ρ) are computed and asterisks denote *p* values less than .05. Each point represents a single storm

among our catchments. In WS2, quickflow generally increased with greater soil moisture, but there was also greater quickflow variability with greater soil moisture (Figure 6a). This pattern is similar in WS2 with respect to groundwater level (Figure 6b). Quickflow dynamics in WS14 were primarily a function of soil moisture, but demonstrated non-unique relationships with groundwater level such that similar levels of groundwater were associated with several different quickflow rates (Figure 6c–d). In SHW, quickflow was a highly non-linear function of soil moisture and groundwater. It is important to note that when the depth to groundwater was less than 500 mm it was interacting with soil moisture measurements (Figure 6e–f). This interaction of measurements contributed to a step change in quickflow when soil moisture values were near 125 mm and to the tight non-linear response of quickflow when soil moisture values were greater than 200 mm.

There were distinct subsurface states differentiating storms occurring below and above the Gross p + ASI threshold in WS2. Frequency distributions in WS2 show soil moisture and groundwater levels were elevated during storms above the threshold (Figure 7a). This wet subsurface state was observed during the highest quickflow observations shown as coloured markers. The trajectory of hourly soil moisture and groundwater measurements over each storm event appeared subnormal to contour lines, which represented the relative subsurface wetness states computed as the ratio of soil moisture to groundwater level (Figure 7a). Overall, this led to a positive, non-linear relationship between quickflow with soil moisture and groundwater.

Soil moisture and groundwater levels in WS14 were decoupled leading to subsurface states that were similar for storms below and above the threshold. Frequency distributions of groundwater levels for storms below versus storms above the threshold were comparable (Figure 7b). Groundwater levels in WS14 were deep even during the wettest soil moisture conditions, and soil moisture varied significantly within this relatively narrow groundwater range. In general, there is a greater frequency of wet soil moisture conditions for storms events above the threshold as shown in the frequency distribution. Even in WS14, quickflows above the 75th percentile were associated with high soil moisture and relatively small rises in groundwater as shown by their clustering around ratio contour lines.

Shallow unsaturated and saturated zone measurements in SHW were decoupled when groundwater was deeper than 600 mm and became tightly coupled as rapid quickflow generation occurred. There was a pronounced shift in subsurface state from storms below the threshold to those above the threshold demonstrated by frequency distributions of soil moisture and groundwater (Figure 7c). Median soil moisture was greater for quickflow producing storms and groundwater distributions were highly skewed in opposite directions demonstrating wet and dry attractor states. Almost all storms above the threshold had groundwater levels within the top 600 mm of the surface and almost all storms below the threshold had groundwater levels deeper than 1 m. The 75th percentile of quickflows at SHW only occurred when groundwater was within 0.5 m of the surface, and it was interacting with soil moisture measurements. The trajectory of hourly soil moisture and groundwater over each storm event appeared independent of the ratio contour lines, which contrasted observations in CHL.

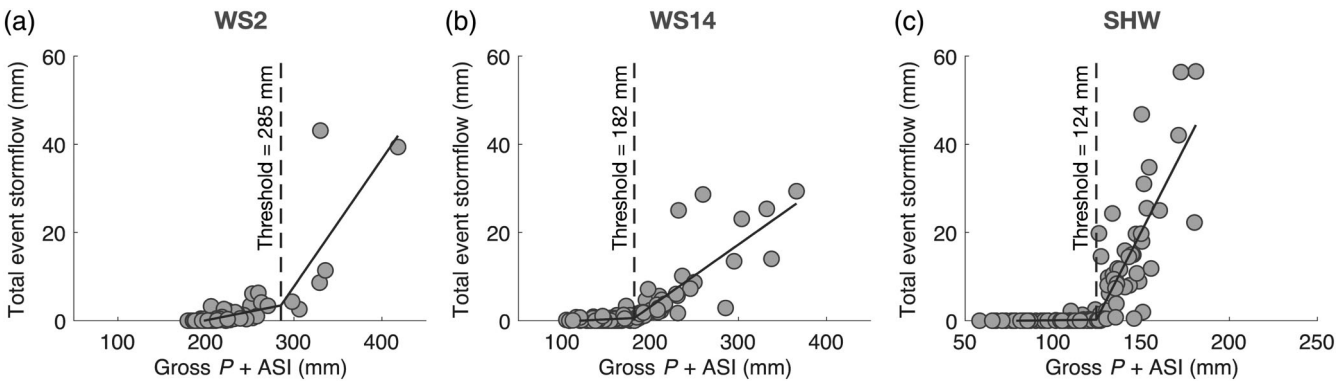

FIGURE 4 Total event stormflow with respect to the sum of gross precipitation (Gross p) and antecedent soil moisture index (ASI) for (a) Watershed 2 (WS2), (b) WS14, and (c) SHW. Piecewise regression analysis derived thresholds are shown as vertical dashed lines and regressions are shown as solid lines. Each symbol denotes a single storm event

TABLE 3 Summary of results from the piecewise regression analysis for each catchment showing the adjusted R^2, the computed threshold, and the mean and standard error of slope parameters for regressions below (m_1) and above (m_2) the threshold shown in Figure 4

	Adjusted R^2	Threshold	m_1	m_2
WS2	0.72	285.19 ± 9.95	0.04 ± 0.02	0.29 ± 0.03
WS14	0.74	181.61 ± 4.90	0.009 ± 0.01	0.14 ± 0.008
SHW	0.73	124.47 ± 2.09	0.004 ± 0.04	0.78 ± 0.06

Two-sample *t*-tests comparing the relative change of soil moisture and groundwater from storm initiation to peak quickflow showed that the subsurface response in WS2 was significantly greater for storms above the threshold than below it (*t*-statistic = 3.96, *p*-value = .005). This difference was not significant in WS14 (*t*-statistic = 1.13, *p*-value = .26). In SHW, the highly non-linear response prevented meaningful comparison between relative subsurface responses using this method.

Capturing the shallow subsurface state using the ratio of shallow soil moisture to groundwater produced non-linear relationships with

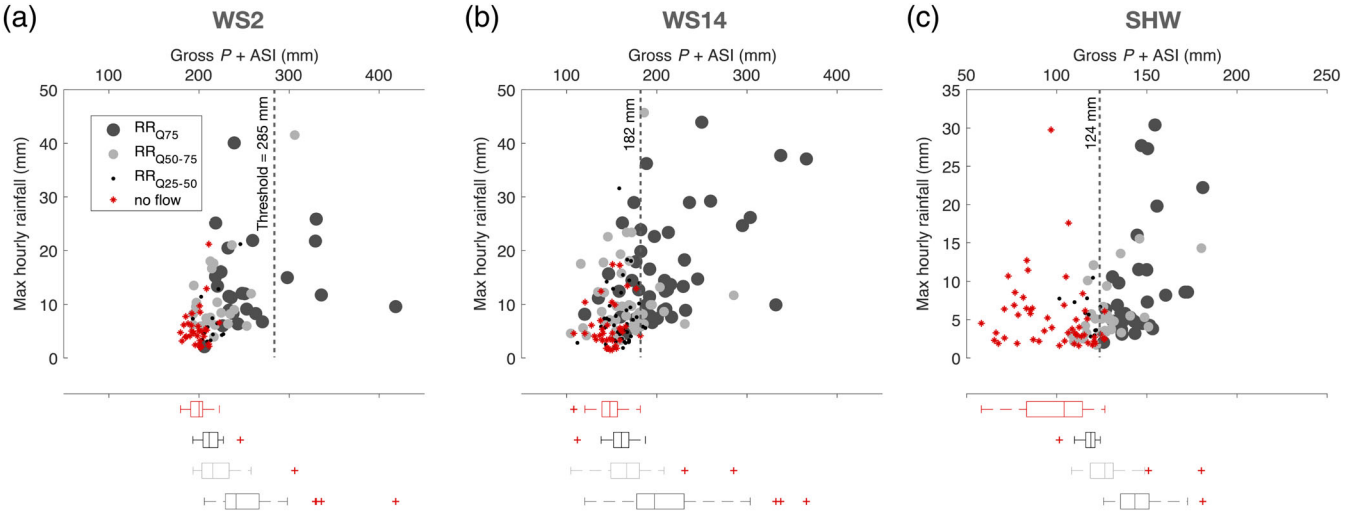

FIGURE 5 Stormflow thresholds using maximum hourly rainfall and the sum of Gross *p* and ASI for (a) WS2, (b) WS14, and (c) SHW following Saffarpour et al., 2016. Markers denote storm events and marker size denotes runoff ratio (RR) divided into quartiles

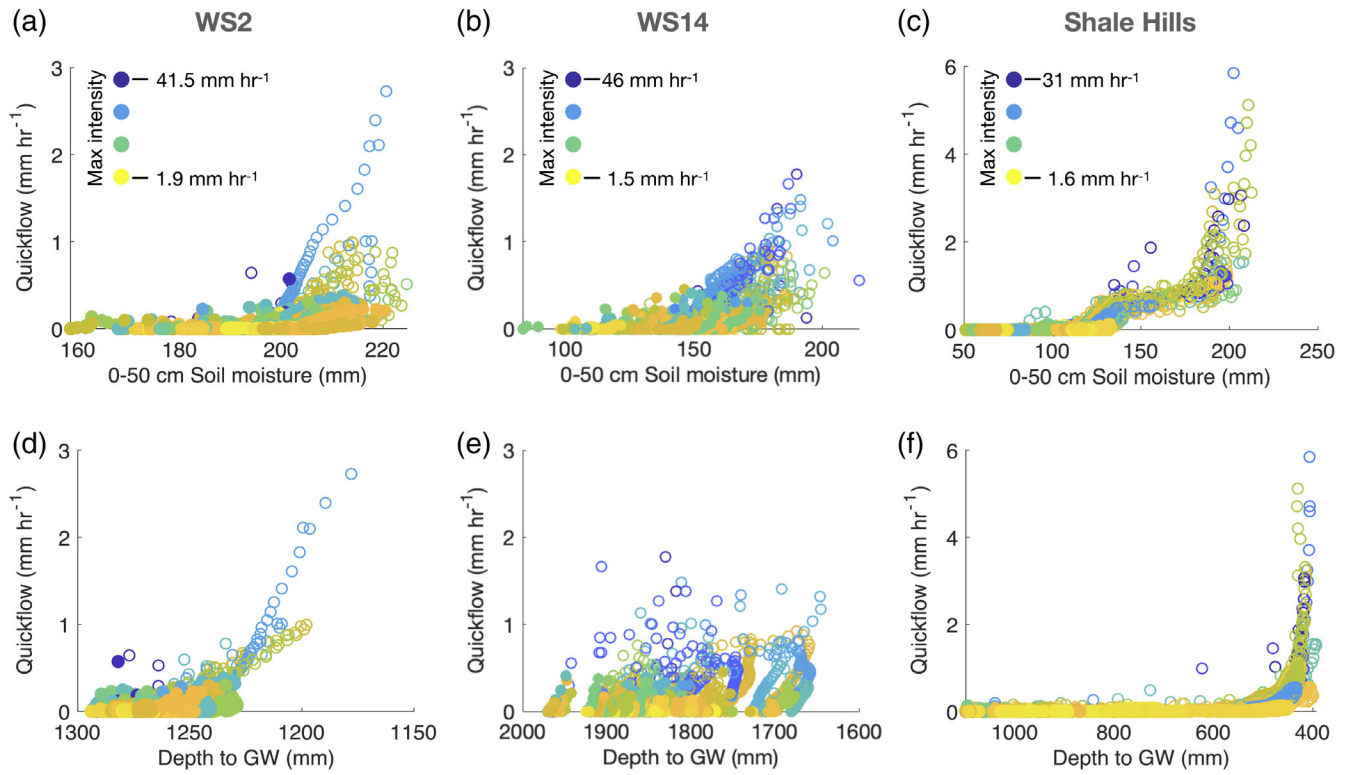

FIGURE 6 The relationship between 0 and 50 cm soil moisture and quickflow (a–c) and the depth to groundwater (GW) and quickflow (d–f) for WS2, WS14, and SHW. The colour shows the relative maximum rainfall intensity observed during each storm event, where blue is the greatest and yellow is the lowest. Each point above represents a single hour within a storm event, which together form multi-hour storm events. Open circles represent storms that are above the threshold identified in Table 3 and solid circles represent points below the threshold

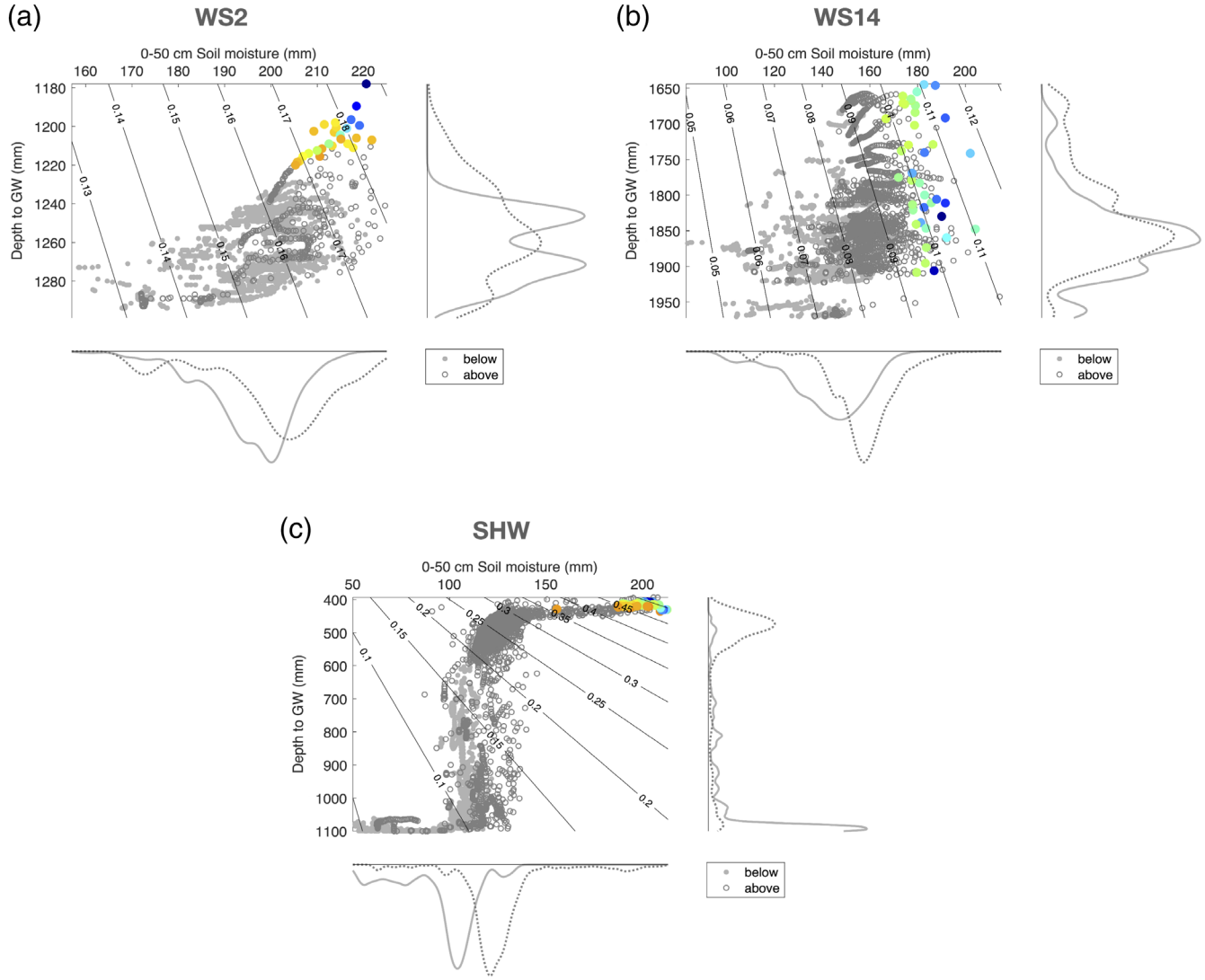

FIGURE 7 Depth to groundwater (mm) with respect to 0–50 cm soil moisture for all storm events in (a) WS2, (b) WS14, and (c) SHW. Contour lines represent the ratio of 0–50 cm soil moisture to depth to groundwater. Each point denotes a single hour and the colours show the 75th percentile of quickflows measured. Blue colours denoting the highest flows and orange the lowest. Open circles represent storms that are above the threshold identified in Table 3 and solid circles represent points below the threshold. Histograms show the density of observations for soil moisture and groundwater in storms above (dashed line) and below (solid line) the threshold

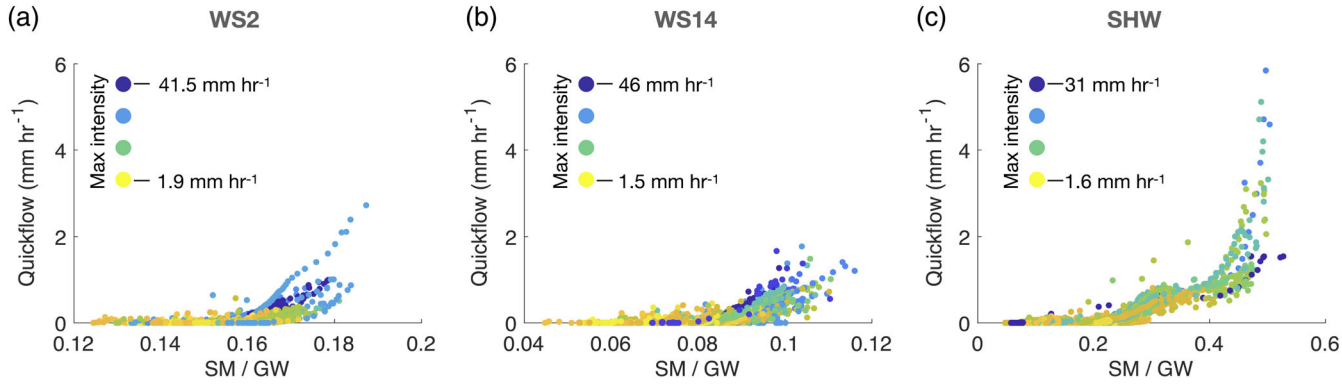

FIGURE 8 The ratio of 0–50 cm soil moisture (SM) to depth to groundwater (GW) for all storms plotted against quickflow for (a) WS2, (b) WS14, and (c) SHW. Each point denotes a single hour and colours represent the maximum hourly rainfall intensity observed during that storm

hourly quickflow for all three sites (Figure 8). In WS2 and WS14, these relationships resembled piecewise linear regressions and in SHW, they formed a single non-linear relationship. Below, we discuss the implications of quantifying quickflow with respect to subsurface states and its limitations.

4 | DISCUSSION

4.1 | Lack of rainfall intensity driven runoff

The impacts of maximum rainfall intensity on quickflow totals were dampened in our study supporting an abundance of previous literature in similarly humid, forested sites. This includes work by Hewlett et al. (1984) showing that peak flows and total stormflow depths at CHL were explained primarily by Gross p and antecedent wetness conditions but not maximum rainfall intensity. Their research was in contrast to seminal work by Dunne and Black (1970) in a humid, forested catchment in Vermont demonstrating that runoff from VSAs was strongly a function of rainfall intensity leading to overland flow. Saffarpour et al. (2016) demonstrated, in part, both runoff models by examining the evolution of multiple thresholds due to (a) Gross p + ASI and (b) maximum hourly rainfall intensity. In their study, there was a clear separation between storm events that generated flow and those that did not. This threshold could be defined by a linear function of Gross p + ASI and maximum hourly rainfall intensity. Our analysis supported the formation of thresholds as a result of Gross p + ASI, but it did not provide strong evidence of rainfall intensity thresholds in our catchments using this method. In Figure 5, the separation between flow and no flow storms was not identifiable in WS2 and WS14. However, in SHW, there was a distinct divide between flow producing storms, but this divide was independent of maximum hourly rainfall intensity. Even among the highest intensity storms in SHW, there were still conditions in which quickflow was not produced, suggesting that this disparity between flow producing storms was driven primarily by ASI, rainfall depth, or both, but not solely rainfall intensity.

Colluvial, forested soils overlying deeply weathered saprolite, like those observed around CHL, have average saturated hydraulic conductivities around 63 mm hr^{-1} that vary between 30 mm hr^{-1} and over 100 mm hr^{-1} (Price et al., 2010). Conductivities for pasture sites in similar soil textures only range from 3 to 25 mm hr^{-1}, leading to rainfall intensity driven quickflow generation via overland flow in pasture sites similar to Saffarpour et al. (2016). Most rainfall rates observed during our study period at CHL were well below the soil conductivities reported in Price et al. (2010). At SHW, minimum saturated hydraulic conductivities measured in the top 50 cm of soils associated with areas of topographically convergent hillslopes and riparian zones varied between 22.8 and 142.2 mm hr^{-1}, respectively (Lin et al., 2006). Of 124 storms analysed, only five had rainfall rates exceeding the minimum conductivities in these soil types. It is important to note that soil heterogeneity may contribute to a high degree of spatial variation in saturated hydraulic conductivities even within a single soil type. Assuming previously published research captures the average soil properties we speculate that under specific antecedent conditions, high-intensity rainfall may trigger VSA behaviour via infiltration excess overland flow in the riparian hollows of SHW due to lower conductivities relative to CHL catchments.

High-intensity events may also activate preferential flow (Anderson, Weiler, Alila, & Hudson, 2009) impacting groundwater levels while bypassing the shallow subsurface resulting in little to no measurable increase in soil moisture (Saffarpour et al., 2016). There was little evidence of rainfall intensity driven preferential bypass from the shallow subsurface to groundwater at CHL in our analyses (Figure 6). At SHW, there were events that triggered groundwater response without similar soil moisture responses, but these were not solely related to intensity (Figure 6f).

Quickflow totals and maximum hourly rainfall intensity capture a single set of metrics for correlating and measuring runoff response. A recent study examining the variability of flow response with respect to several metrics across catchments in Canada, New Zealand, Australia, and the US found that the combination of storage and intensity metrics explained more variance in flow magnitude and timing than storage alone (Ross, Ali, Spence, Oswald, & Casson, 2019). Our analysis found that correlations with maximum hourly rainfall intensity were weak compared to correlations with Gross p but not negligible. Including additional intensity metrics like average rainfall intensity which characterize intensity and storm length simultaneously may capture a relatively stronger impact of intensity on quickflow totals.

4.2 | Non-linear runoff linked to soil moisture–groundwater coupling

Over a single storm, the strength of soil moisture–groundwater coupling may signal transitions between shallow and deeper subsurface flow generation, while the shape of soil moisture–groundwater relationships over many storms may indicate predominate catchment-wide runoff mechanisms. The wet-up of both soil moisture and groundwater have been separately linked to threshold changes in streamflow generation. For example, Penna, Borga, Norbiato, and Fontana (2009) showed that rapidly rising flows in a steeply sloping catchment of the Italian Alps were associated with soil moisture measurements above 45%. Groundwater dynamics were dampened during drier periods and responded with soil moisture only under the largest storms. McGlynn and McDonnell (2003) hypothesised that low flows were primarily saturation excess overland flow in riparian areas, but as VSAs expanded and connected to hillslopes during large storms flow quickly increased due to a supply of subsurface flows from the hillslope.

At CHL, early experiments suggested shallow throughflow and recharge triggers translatory flow that provides sufficient quickflow response (Hewlett & Hibbert, 1967), while baseflow was supplied by a slower travelling pulse of soil moisture downslope (Hewlett, 1961;

Hewlett & Hibbert, 1963). Recent work suggested that flow generation was more complex at CHL and that soil moisture response versus groundwater response was sensitive to storm event size (Singh et al., 2018b) similar to McGlynn and McDonnell (2003). In our analysis, WS14 and even more so WS2 showed relatively stable groundwater levels that coupled with rising soil moisture only under the wettest conditions (Figure 7). In WS2, this coupling was greatest during storms that also generated the highest flows, and coupling during these storms was significantly greater than storms that fell below the threshold. Even under these relatively wet conditions, flow may still be dominated by shallow unsaturated through flow because frequency distributions of groundwater in Figure 7a were similar for storm events above and below thresholds.

The distinction between coupling and decoupling of subsurface responses and quickflow generation was weaker in WS14 than in WS2. This lack of distinction in WS14 could be due, in part, to the method used to identify thresholds that may have included too many small storms (Figure 4). The overall shape of the soil moisture and groundwater relationship in WS14 may also contribute to a lack of distinction. Unlike WS2, the relationship in WS14 cannot be defined by a single function, which suggests there exist several subsurface conditions that generate similar flows. This non-unique behaviour can be driven by the temporal scales at which soil moisture and groundwater respond. In WS14, groundwater variation was dominated by seasonal fluctuations while soil moisture was dominated by storm event scale fluctuations.

Soil moisture and groundwater in SHW were almost entirely decoupled except when water table levels were within 600 mm of the surface (Figure 7c). Coupling under high water table levels at SHW reflects an interaction of groundwater with soil moisture measurements made at a depth of 500 mm rather than a separate but simultaneous wet-up of soil moisture and groundwater. This suggests that quickflow response was largely a function of groundwater level rather than soil moisture or the interaction of the two as shown at CHL. The highly non-linear relationship between groundwater and soil moisture makes comparing the degree of coupling between storms above and below the threshold difficult (Figure 7c); however, the bimodal distributions may suggest the existence of a two state system. Grayson, Western, Chiew, and Blöschl (1997) contrasted periods when spatial soil moisture was organized with respect to topography versus when it was random as 'two preferred states'. Under a wet and spatially organized state there was greater lateral and vertical redistribution of water than under a dry state. Comparisons can be drawn between wet and dry states and processes like hillslope connection and disconnection particularly to riparian areas (Jencso et al., 2009; McGlynn & McDonnell, 2003; McGlynn & Seibert, 2003) that lead to non-linear quickflow response. At SHW, the rapid transition from dry to wet conditions that contributed to quickflow generation indicates the activation of runoff generation processes, discussed below, and potentially the connection of the riparian area to the hillslope. In the following section, we further discuss the implications of subsurface coupling for identifying runoff processes.

4.3 | Soil moisture, groundwater dynamics help detect runoff mechanisms

Based on our findings of subsurface coupling at CHL, the translatory flow model may be too simplistic for explaining non-linear quickflow generation, and perhaps we need to consider several co-occurring runoff processes that vary with respect to subsurface state. In WS14, quickflow response and Gross p + ASI thresholds absent of significant groundwater coupling may suggest matric and pipe flow activation under high antecedent wetness conditions and large storms (Sidle et al., 2000). Matric and pipe flow in humid forested catchments are highly dependent on rainfall depth and antecedent wetness and when activated can contribute significantly to rapidly rising quickflows (Meerveld & McDonnell, 2006a, 2006b; Uchida et al., 2005; Uchida, Kosugi, & Mizuyama, 2002). Other mechanisms that contribute to non-linear quickflow response may include flow along the bedrock interface. At CHL, there is a deep, highly permeable saprolite layer beneath the soil (Hatcher, 1988). Rapid vertical drainage in this layer may eventually transition to lateral flows along the bedrock interface leading to non-linear quickflow response formed by bedrock topography (Band et al., 2014) and fill-and-spill mechanisms (Meerveld & McDonnell, 2006b; Uchida et al., 2001, 2005). When these deep lateral flows connect to riparian areas, they can drive rapid quickflow generation (Figure 4) without generating significant groundwater response (Figure 7). Pairing thresholds analyses with high-resolution soil moisture and groundwater data help supplement the translatory flow model by providing indicators of specific runoff mechanisms.

Subsurface behaviour in WS2 was similar, but stronger soil moisture and groundwater coupling under wet conditions indicated greater groundwater contributions to quickflow relative to WS14. Singh et al. (2018b) quantified variables driving shallow groundwater rise across catchments at CHL supporting differences observed in the strength of soil moisture–groundwater coupling between WS2 and WS14. They found several interacting drivers of groundwater rise including aspect, season, local slope, topographic position, Gross p, and antecedent groundwater levels. Drier south-facing catchments like WS2 required greater Gross p to trigger groundwater response compared to north-facing catchments like WS14, but local slope became as important as Gross p during the dormant season. Slopes across WS2 and WS14 are comparable (Table 1), but the local slopes at well installations are greater in WS2 (25.6°) than WS14 (20.8°). Trade-offs between temporal and local geomorphic drivers of groundwater response likely contributed to seasonal groundwater signals in WS14 versus storm-event groundwater signals in WS2. Groundwater contributions to quickflow may also be underestimated in both watersheds when inflow to the saturated zone was equal to outflow to the stream. These conditions produce no measurable change in groundwater level despite an increase in streamflow. Equal inflow and outflow rates may reflect transition periods between slower and more rapid quickflow changes.

At the catchment scale, the Coweeta Basin is also intersected by a large thrust fault such that WS2 is situated in a different lithology than where measurements are made in WS14 (Hatcher, 1988). As a

result, the stream morphology in WS14 transitions from rocky steep channels similar to WS2 below the thrust fault to relatively gently sloped channels and banks above it. We speculate that groundwater level and soil moisture–groundwater coupling may more closely resemble WS2 below the thrust fault. Lithology may also contribute to other catchment-wide differences in properties like wetted stream lengths (Jensen, McGuire, & Prince, 2017) or curvature driving well responsiveness (Bachmair & Weiler, 2014; Singh et al., 2018b).

The decoupled subsurface response and high dependence on groundwater for flow generation at SHW are consistent with transmissivity feedbacks observed in other thinly soiled catchments like Hubbard Brook (Detty & McGuire, 2010). Lin et al. (2006) found conductivities greater than 100 mm hr^{-1} in soils throughout SHW at depths less 0.5 m that declined with depth. This resulted in rapid recharge to the groundwater, which may explain large water table fluctuations observed in our study. Using 10 min data, Lin and Zhou (2008) showed complex subsurface response during a typical rain event in the riparian hollows of SHW. Soil moisture rapidly responded to precipitation in the form of a wetting front starting at the surface and percolating deeper. As rainfall subsided, soil moisture remained elevated or decreased due to drainage. A delayed response of groundwater levels and deeper preferential flows from an adjacent hillslope caused soil moisture to re-saturate but from the bottom-up. They found that this two-stage response was dependent on intensity, antecedent conditions, and landscape position, but the implications on quickflow generation were not fully considered in their study. Our results suggest that this initial surface soil wetting may not contribute significantly to quickflow generation compared to the groundwater response. This further suggests that as the groundwater rises into more highly conductive soils water is more effectively transmitted to the stream. Overland flow unlikely occurred during the measurement period as riparian groundwater levels never reached the surface.

These findings have implications for the T^3 template (Buttle, 2006), which describes the relative role of network connectivity (topology), vertical versus lateral partitioning (typology), and hydraulic gradients (topography) on controlling streamflow generation. Our study suggests that topography is a first-order control of streamflow in WS2 and WS14, but that topological differences driven by lithology may exert a secondary control. On the other hand, SHW may be secondarily controlled by vertical versus lateral partitioning. This leads to subsurface dynamics and streamflow generation that are dominated by changes in groundwater level.

4.4 | Do simple storage–flux relationships form irrespective of dominant runoff processes?

Duffy (1996) described the formulation of a simple model using unsaturated and saturated volumes to derive flow based on a steady-state saturated–unsaturated flow model. In this storage–flux model, streamflow was only generated by subsurface storage and infiltration excess precipitation. Unsaturated and saturated volumes were coupled and produced an inverse relationship such that as the ratio of unsaturated to saturated volumes decreased total flow increased. It is important to note that our characterisation of the unsaturated zone only quantifies water volume in the top 50 cm rather than to the water table diminishing the hypothesised inverse relationship. As a result, relationships between soil moisture and groundwater were variable between catchments and in some cases were non-unique and decoupled (e.g., WS14). Despite differences in the degree of coupling between our catchments, the relative ratios of shallow soil moisture to groundwater may provide sufficient information for explaining the amount of quickflow generated (Figure 8).

Duffy's (1996) model also characterised the unsaturated and saturated zones across the entire catchment. Replicating this experiment requires more measurements than were available for our study, but our analysis showed that using coincident, riparian measurements in topographically convergent locations may sufficiently integrate behaviour from upslope. A major assumption of our study was that these near stream measurements vary through time in ways correlated to that of the whole watershed. Information from these representative sites may be sufficient for understanding flow processes contributing to non-linear quickflow responses at the catchment outlet.

Our analysis could benefit from additional studies that examine coupling and decoupling of soil moisture and groundwater and how these relationships change with respect to topographic position. It is important that future work use coincident measurements of groundwater and soil moisture because large offsets even in flatter terrain could dramatically alter these relationships. Findings from this study should also be tested in catchments where dominant runoff mechanisms have been identified (e.g., Panola Research Watershed or Hubbard Brook). We should further design future experiments that integrate unsaturated moisture to the depth of the groundwater in riparian areas to more directly explore the model Duffy (1996) proposed, which requires installing probes deep enough to intersect transient groundwater levels.

5 | CONCLUSIONS

From our analysis, we conclude the following:

1 Maximum hourly rainfall intensity had a relatively small effect on quickflow generation compared to Gross p or Gross p + ASI in forested, headwater catchments analysed in this study. This was due in part to high saturated hydraulic conductivities that allow for rapid infiltration and transmission to the stream via preferential flow, matric flow, or recharge into the groundwater.
2 Soil moisture and groundwater measurements supplemented thresholds analyses of quickflow by serving as additional indicators of runoff mechanisms. The degree of coupling between soil moisture and groundwater and their relative response during storms varied across forested, headwater catchments and was associated with runoff generation mechanisms unique to the hillslope or catchment.

3 Near stream measurements of co-located soil moisture and groundwater levels that integrate upslope behaviour may be sufficient for empirically characterising non-linear flow response at the catchment outlet, but more research is needed examining how the generalisability of these results.

ACKNOWLEDGEMENTS

We acknowledge the support of the USDA Forest Service for providing hydrologic and climate data and the assistance of USDA Forest Service and Long-Term Ecological Research (LTER) staff with installing and collecting in situ soil moisture measurements. We also acknowledge the Susquehanna Shale Hills Critical Zone Observatory and their staff for collecting and providing data through their open data policy. This study was supported by the USDA Forest Service, Southern Research Station, and by NSF grants DEB8012093, DEB8706444, DEB9011661, DEB0218001, DEB0823293, DBI-1226983, DEB-1440485, and DEB-1637522 to the Coweeta LTER program at the University of Georgia. Financial support was also provided by NSF grants EAR-0725019, EAR-1239285, EAR-1331726 awarded to the Susquehanna Shale Hills Critical Zone. Logistical support and/or data were provided by the NSF-supported Shale Hills Susquehanna Critical Zone Observatory.

DATA AVAILABILITY STATEMENT

Precipitation and discharge data from Coweeta Hydrologic Laboratory are available by request from the USDA Forest Service Southern Research Station. Groundwater stage and soil moisture data are available through the Coweeta LTER data catalogue (https://coweeta.uga.edu/dbpublic/data_catalog.asp) accession number 4048 and 4049 and from Singh, Emanuel, Nippgen, McGlynn, (2018a). All data from Shale Hills can be found online and links to data are provided in the references (see Arthur, 2016; Duffy, 2012a, 2012b, 2012c).

ORCID

Charles I. Scaife https://orcid.org/0000-0002-7776-1815

REFERENCES

Anderson, A., Weiler, M., Alila, Y., & Hudson, R. (2009). Subsurface flow velocities in a hillslope with lateral preferential flow. *Water Resources Research*, *45*(11), W11407. https://doi.org/10.1029/2008wr007121

Arthur, D. K. (2016). "CZO Dataset: Shale Hills - Precipitation, Meteorology (2009–2016)." Retrieved on November 21, 2019 from http://criticalzone.org/shale-hills/data/dataset/4940/

Bachmair, S., & Weiler, M. (2014). Interactions and connectivity between runoff generation processes of different spatial scales. *Hydrological Processes*, *28*(4), 1916–1930. https://doi.org/10.1002/hyp.9705

Band, L., McDonnell, J., Duncan, J., Barros, A., Bejan, A., Burt, T., … Troch, P. A. (2014). Ecohydrological flow networks in the subsurface. *Ecohydrology*, *7*(4), 1073–1078. https://doi.org/10.1002/eco.1525

Berg, T. M., Edmunds, W. E., Geyer, A. R., Glover, A. D., Hoskins, D. M., MacLachlan, D. B., …, & Socolow, A. A. (compilers) 1980. *Geologic map of Pennsylvania. 4th Ser., map 1*. Pennsylvania Geological Survey, Harrisburg, PA

Brantley, S. L., White, T., West, N., Williams, J. Z., Forsythe, B., Shapich, D., … Gu, X. (2019). Susquehanna Shale Hills critical zone observatory: Shale Hills in the context of Shaver's Creek Watershed. *Vadose Zone Journal*, *17*(1), 1–19. https://doi.org/10.2136/vzj2018.04.0092

Brocca, L., Morbidelli, R., Melone, F., & Moramarco, T. (2007). Soil moisture spatial variability in experimental areas of Central Italy. *Journal of Hydrology*, *333*(2-4), 356–373. https://doi.org/10.1016/j.jhydrol.2006.09.004

Burt, T., Miniat, C., Laseter, S., & Swank, W. (2018). Changing patterns of daily precipitation totals at the Coweeta hydrologic laboratory, North Carolina, USA. *International Journal of Climatology*, *38*(1), 94–104. https://doi.org/10.1002/joc.5163

Buttle, J. M. (2006). Mapping first-order controls on streamflow from drainage basins: The T3 template. *Hydrological Processes*, *20*(15), 3415–3422. https://doi.org/10.1002/hyp.6519

Buttle, J. M., Dillon, P., & Eerkes, G. (2004). Hydrologic coupling of slopes, riparian zones and streams: An example from the Canadian shield. *Journal of Hydrology*, *287*(1–4), 161–177. https://doi.org/10.1016/j.jhydrol.2003.09.022

Buttle, J. M., Webster, K. L., Hazlett, P. W., & Jeffries, D. S. (2019). Quickflow response to forest harvesting and recovery in a northern hardwood forest landscape. *Hydrological Processes*, *33*(1), 47–65. https://doi.org/10.1002/hyp.13310

Daly, C., Slater, M., Roberti, J., Laseter, S., & Swift, L. (2017). High-resolution precipitation mapping in a mountainous watershed: Ground truth for evaluating uncertainty in a national precipitation dataset. *International Journal of Climatology*, *37*(S1), 124–137. https://doi.org/10.1002/joc.4986

Day, F. P., Phillips, D. L., & Monk, C. D. (1988). Forest communities and patterns. In W. T. Swank & D. A. Crossley (Eds.), *Forest hydrology and ecology at Coweeta. Ecological Studies (Analysis and Synthesis)* (Vol. 66). New York, NY: Springer.

Detty, J., & McGuire, K. (2010). Threshold changes in storm runoff generation at a till-mantled headwater catchment. *Water Resources Research*, *46*(7), W07525. https://doi.org/10.1029/2009wr008102

Duffy, C. J. (1996). A two-state integral-balance model for soil moisture and groundwater dynamics in complex terrain. *Water Resources Research*, *32*(8), 2421–2434. https://doi.org/10.1029/96wr01049

Duffy, Christopher J. (2012a). "CZO Dataset: Shale Hills - Groundwater Depth (2009–2012) - Shale Hills Groundwater Depth Data." Retrieved on November 21, 2019 from http://criticalzone.org/shale-hills/data/dataset/3614/

Duffy, Christopher J. (2012b). "CZO Dataset: Shale Hills - Soil Moisture (2009–2012) - Shale Hills RTH Soil Moisture Data." Retrieved on November 21, 2019 from http://criticalzone.org/shale-hills/data/dataset/3615/

Duffy, Christopher J. (2012c). "CZO Dataset: Shale Hills - Streamflow / Discharge (2006–2012) - Shale Hills Stream Flow/Discharge Data." Retrieved on November 21, 2019 from http://criticalzone.org/shale-hills/data/dataset/3613/

Dunne, T., & Black, R. D. (1970). Partial area contributions to storm runoff in a small New England watershed. *Water Resources Research*, *6*(5), 1296–1311. https://doi.org/10.1029/wr006i005p01296

Elliott, K. J., Vose, J. M., Swank, W. T., & Bolstad, P. V. (1999). Long-term patterns in vegetation-site relationships in a Southern Appalachian Forest. *Journal of the Torrey Botanical Society*, *126*(4), 320–324. https://doi.org/10.2307/2997316

Freer, J., McDonnell, J., Beven, K., Peters, N., Burns, D., Hooper, R., … Kendall, C. (2002). The role of bedrock topography on subsurface storm flow. *Water Resources Research*, *38*(12), 1269. https://doi.org/10.1029/2001wr000872

Fu, C., Chen, J., Jiang, H., & Dong, L. (2013). Threshold behavior in a fissured granitic catchment in southern China: 2. Modeling and uncertainty analysis. *Water Resources Research*, *49*(5), 2536–2551. https://doi.org/10.1002/wrcr.20193

Grayson, R., & Western, A. (1998). Towards areal estimation of soil water content from point measurements: Time and space stability of mean

response. *Journal of Hydrology*, *207*(1–2), 68–82. https://doi.org/10.1016/s0022-1694(98)00096-1

Grayson, R. B., Western, A. W., Chiew, F. H., & Blöschl, G. (1997). Preferred states in spatial soil moisture patterns: Local and nonlocal controls. *Water Resources Research*, *33*(12), 2897–2908. https://doi.org/10.1029/97wr02174

Haga, H., Matsumoto, Y., Matsutani, J., Fujita, M., Nishida, K., & Sakamoto, Y. (2005). Flow paths, rainfall properties, and antecedent soil moisture controlling lags to peak discharge in a granitic unchanneled catchment. *Water Resources Research*, *41*, W12410. https://doi.org/10.1029/2005WR004236

Hatcher, R. D. (1988). Bedrock geology and regional geologic setting of Coweeta hydrologic Laboratory in the Eastern Blue Ridge. In W. T. Swank & D. A. Crossley (Eds.), *Forest hydrology and ecology at Coweeta. Ecological Studies (Analysis and Synthesis)* (Vol. 66). New York, NY: Springer.

Hewlett, J., Fortson, J., & Cunningham, G. (1984). Additional tests on the effect of rainfall intensity on storm flow and peak flow from wild-land basins. *Water Resources Research*, *20*(7), 985–989. https://doi.org/10.1029/wr020i007p00985

Hewlett, J. D. (1961). *Soil moisture as a source of base flow from steep mountain watersheds*. Asheville, NC: Southeastern Forest Experiment Station, US Department of Agriculture, Forest Service.

Hewlett, J. D., & Hibbert, A. R. (1963). Moisture and energy conditions within a sloping soil mass during drainage. *Journal of Geophysical Research*, *68*(4), 1081–1087. https://doi.org/10.1029/jz068i004p01081

Hewlett, J. D., & Hibbert, A. R. (1967). Factors affecting the response of small watersheds to precipitation in humid areas. *Forest Hydrology*, *1*, 275–290.

Horton, R. E. (1933). The role of infiltration in the hydrologic cycle. *EOS, Transactions American Geophysical Union*, *14*(1), 446–460. https://doi.org/10.1029/tr014i001p00446

Hrachowitz, M., Savenije, H. H. G., Blöschl, G., McDonnell, J. J., Sivapalan, M., Pomeroy, J. W., … Cudennec, C. (2013). A decade of predictions in Ungauged basins (PUB)—A review. *Hydrological Sciences Journal*, *58*(6), 1198–1255. https://doi.org/10.1080/02626667.2013.803183

Jencso, K. G., McGlynn, B. L., Gooseff, M. N., Wondzell, S. M., Bencala, K. E., & Marshall, L. A. (2009). Hydrologic connectivity between landscapes and streams: Transferring reach- and plot-scale understanding to the catchment scale. *Water Resources Research*, *45*, W04428. https://doi.org/10.1029/2008WR007225

Jensen, C. K., McGuire, K. J., & Prince, P. S. (2017). Headwater stream length dynamics across four physiographic provinces of the Appalachian highlands. *Hydrological Processes*, *31*(19), 3350–3363. https://doi.org/10.1002/hyp.11259

Kirchner, J. W. (2009). Catchments as simple dynamical systems: Catchment characterization, rainfall-runoff modeling, and doing hydrology backward. *Water Resources Research*, *45*, W02429. https://doi.org/10.1029/2008WR006912

Laseter, S. H., Ford, C. R., Vose, J. M., & Swift, L. W. (2012). Long-term temperature and precipitation trends at the Coweeta hydrologic laboratory, Otto, North Carolina, USA. *Hydrology Research*, *43*(6), 890–901. https://doi.org/10.2166/nh.2012.067

Lehmann, P., Hinz, C., McGrath, G., Meerveld, T. H., & McDonnell, J. J. (2007). Rainfall threshold for hillslope outflow: An emergent property of flow pathway connectivity. *Hydrology and Earth System Sciences*, *11*(2), 1047–1063. https://doi.org/10.5194/hess-11-1047-2007

Lin, H. (2006). Temporal stability of soil moisture spatial pattern and subsurface preferential flow pathways in the Shale Hills catchment. *Vadose Zone Journal*, *5*(1), 317–340. https://doi.org/10.2136/vzj2005.0058

Lin, H., Kogelmann, W., Walker, C., & Bruns, M. (2006). Soil moisture patterns in a forested catchment: A hydropedological perspective. *Geoderma*, *131*(3–4), 345–368. https://doi.org/10.1016/j.geoderma.2005.03.013

Lin, H., & Zhou, X. (2008). Evidence of subsurface preferential flow using soil hydrologic monitoring in the Shale Hills catchment. *European Journal of Soil Science*, *59*(1), 34–49. https://doi.org/10.1111/j.1365-2389.2007.00988.x

McDonnell, J. J. (1990). A rationale for old water discharge through macropores in a steep, humid catchment. *Water Resources Research*, *26*(11), 2821–2832. https://doi.org/10.1029/wr026i011p02821

McGlynn, B. L., & McDonnell, J. J. (2003). Quantifying the relative contributions of riparian and hillslope zones to catchment runoff. *Water Resources Research*, *39*(11), 1310. https://doi.org/10.1029/2003wr002091

McGlynn, B. L., McDonnell, J. J., Seibert, J., & Kendall, C. (2004). Scale effects on headwater catchment runoff timing, flow sources, and groundwater-streamflow relations. *Water Resources Research*, *40*, W07504. https://doi.org/10.1029/2003wr002494

McGlynn, B. L., & Seibert, J. (2003). Distributed assessment of contributing area and riparian buffering along stream networks. *Water Resources Research*, *39*(4), 1082. https://doi.org/10.1029/2002wr001521

Meerveld, T. H., & McDonnell, J. J. (2006a). Threshold relations in subsurface stormflow: 1. A 147-storm analysis of the Panola hillslope. *Water Resources Research*, *42*(2), W02410. https://doi.org/10.1029/2004wr003778

Meerveld, T. H., & McDonnell, J. J. (2006b). Threshold relations in subsurface stormflow: 2. The fill and spill hypothesis. *Water Resources Research*, *42*(2), W02411. https://doi.org/10.1029/2004wr003800

Miller, D., Miniat, C., Wooten, R., & Barros, A. (2019). An expanded investigation of atmospheric Rivers in the southern Appalachian Mountains and their connection to landslides. *Atmosphere*, *10*(2), 71. https://doi.org/10.3390/atmos10020071

Mosley, P. M. (1979). Streamflow generation in a forested watershed, New Zealand. *Water Resources Research*, *15*(4), 795–806. https://doi.org/10.1029/wr015i004p00795

Mosley, P. M. (1982). Subsurface flow velocities through selected forest soils, South Island, New Zealand. *Journal of Hydrology*, *55*(1–4), 65–92. https://doi.org/10.1016/0022-1694(82)90121-4

Muggeo, V. M. (2003). Estimating regression models with unknown breakpoints. *Statistics in Medicine*, *22*(19), 3055–3071. https://doi.org/10.1002/sim.1545

Nippgen, F., McGlynn, B. L., Emanuel, R. E., & Vose, J. M. (2016). Watershed memory at the Coweeta hydrologic laboratory: The effect of past precipitation and storage on hydrologic response. *Water Resources Research*, *52*(3), 1673–1695. https://doi.org/10.1002/2015wr018196

Penna, D., Borga, M., Norbiato, D., & Fontana, G. (2009). Hillslope scale soil moisture variability in a steep alpine terrain. *Journal of Hydrology*, *364*(3-4), 311–327. https://doi.org/10.1016/j.jhydrol.2008.11.009

Price, K., Jackson, C., & Parker, A. (2010). Variation of surficial soil hydraulic properties across land uses in the southern blue Ridge Mountains, North Carolina, USA. *Journal of Hydrology*, *383*(3–4), 256–268. https://doi.org/10.1016/j.jhydrol.2009.12.041

R Core Team. (2019). *R: A language and environment for statistical computing. R Foundation for Statistical Computing*, Vienna, Austria. http://www.R-project.org/

Ramos-Scharrón, C., & LaFevor, M. (2018). Effects of forest roads on runoff initiation in low-order ephemeral streams. *Water Resources Research*, *54*(11), 8613–8631. https://doi.org/10.1029/2018wr023442

Ross, C., Ali, G., Spence, C., Oswald, C., & Casson, N. (2019). Comparison of event-specific rainfall–runoff responses and their controls in contrasting geographic areas. *Hydrological Processes*, *33*(14), 1961–1979. https://doi.org/10.1002/hyp.13460

Saffarpour, S., Western, A. W., Adams, R., & McDonnell, J. J. (2016). Multiple runoff processes and multiple thresholds control agricultural runoff generation. *Hydrology and Earth System Sciences*, *20*(11), 4525–4545. https://doi.org/10.5194/hess-20-4525-2016

Scaife, C. I., & Band, L. E. (2017). Nonstationarity in threshold response of stormflow in southern Appalachian headwater catchments. *Water Resources Research*, *53*(8), 6579–6596. https://doi.org/10.1002/2017wr020376

Seibert, J., Bishop, K., Rodhe, A., & McDonnell, J. J. (2003). Groundwater dynamics along a hillslope: A test of the steady state hypothesis. *Water Resources Research*, *39*(1), 1014. https://doi.org/10.1029/2002wr001404

Sidle, R. C., Tsuboyama, Y., Noguchi, S., Hosoda, I., Fujieda, M., & Shimizu, T. (2000). Stormflow generation in steep forested headwaters: A linked hydrogeomorphic paradigm. *Hydrological Processes*, *14*(3), 369–385. https://doi.org/10.1002/(sici)1099-1085(20000228)14:3<369::aid-hyp943>3.0.co;2-p

Singh, N. K., Emanuel, R. E., Nippgen, F., McGlynn, B. L., & Miniat, C. F. (2018a). "Groundwater stage for 22 wells and timeseries of rainfall." Retrieved on November 21, 2019 from https://doi.org/10.6084/m9.figshare.6463133.v1

Singh, N. K., Emanuel, R. E., Nippgen, F., McGlynn, B. L., & Miniat, C. F. (2018b). The relative influence of storm and landscape characteristics on shallow groundwater responses in forested headwater catchments. *Water Resources Research*, *54*(12), 9883–9900. https://doi.org/10.1029/2018wr022681

Smith, L., Eissenstat, D., & Kaye, M. (2017). Variability in aboveground carbon driven by slope aspect and curvature in an eastern deciduous forest, USA. *Canadian Journal of Forest Research*, *47*(2), 149–158. https://doi.org/10.1139/cjfr-2016-0147

Spence, C., & Woo, M. (2003). Hydrology of subarctic Canadian shield: Soil-filled valleys. *Journal of Hydrology*, *279*(1-4), 151–166. https://doi.org/10.1016/s0022-1694(03)00175-6

Swank, W., & Douglass, J. (1975). Nutrient flux in undisturbed and manipulated forest ecosystems in the southern Appalachian Mountains. Paper presented at: Proceedings of the Tokyo Symposium in the Hydrological Characteristics of River Basins, International Association of Hydrological Sciences (Tokyo), 445–456.

Swift, L. W., Jr., Cunningham, G. B., & Douglass, J. E. (1988). Climate and hydrology. In W. T. Swank & D. A. Crossley (Eds.), *Forest hydrology and ecology at Coweeta. Ecological Studies (Analysis and Synthesis)* (Vol. 66). New York, NY: Springer.

Teuling, A., Lehner, I., Kirchner, J., & Seneviratne, S. (2010). Catchments as simple dynamical systems: Experience from a Swiss prealpine catchment. *Water Resources Research*, *46*(10), W10502. https://doi.org/10.1029/2009wr008777

Uchida, T., Kosugi, K., & Mizuyama, T. (2001). Effects of pipeflow on hydrological process and its relation to landslide: A review of pipeflow studies in forested headwater catchments. *Hydrological Processes*, *15*(11), 2151–2174. https://doi.org/10.1002/hyp.281

Uchida, T., Kosugi, K., & Mizuyama, T. (2002). Effects of pipe flow and bedrock groundwater on runoff generation in a steep headwater catchment in Ashiu, Central Japan. *Water Resources Research*, *38*(7), 24. https://doi.org/10.1029/2001wr000261

Uchida, T., Meerveld, T. H., & McDonnell, J. J. (2005). The role of lateral pipe flow in hillslope runoff response: An intercomparison of non-linear hillslope response. *Journal of Hydrology*, *311*(1–4), 117–133. https://doi.org/10.1016/j.jhydrol.2005.01.012

Vachaud, G., Silans, P. A., Balabanis, P., & Vauclin, M. (1985). Temporal stability of spatially measured soil water probability density function. *Soil Science Society of America Journal*, *49*(4), 822–828. https://doi.org/10.2136/sssaj1985.03615995004900040006x

Velbel, M. A. (1988). Weathering and soil-forming processes. In W. T. Swank & D. A. Crossley (Eds.), *Forest hydrology and ecology at Coweeta. Ecological Studies (Analysis and Synthesis)* (Vol. 66). New York, NY: Springer.

Weiler, M., & McDonnell, J. (2004). Virtual experiments: A new approach for improving process conceptualization in hillslope hydrology. *Journal of Hydrology*, *285*(1–4), 3–18. https://doi.org/10.1016/s0022-1694(03)00271-3

Wilson, G., Nieber, J., Fox, G., Dabney, S., Ursic, M., & Rigby, J. (2017). Hydrologic connectivity and threshold behavior of hillslopes with fragipans and soil pipe networks. *Hydrological Processes*, *31*(13), 2477–2496. https://doi.org/10.1002/hyp.11212

Wittenberg, H., & Sivapalan, M. (1999). Watershed groundwater balance estimation using streamflow recession analysis and baseflow separation. *Journal of Hydrology*, *219*(1–2), 20–33. https://doi.org/10.1016/s0022-1694(99)00040-2

SUPPORTING INFORMATION

Additional supporting information may be found online in the Supporting Information section at the end of this article.

How to cite this article: Scaife CI, Singh NK, Emanuel RE, Miniat CF, Band LE. Non-linear quickflow response as indicators of runoff generation mechanisms. *Hydrological Processes*. 2020;34:2949–2964. https://doi.org/10.1002/hyp.13780